

RESEARCH

Open Access



Effects of Fe and Zn alone and combined treatment on *Triticum aestivum* L. seed germination

Zhe Zhang^{1†}, Rongrong Ma^{1†}, Yihui Tao¹, Ziling Wang¹ and Yingli Yang^{1*}

Abstract

Seed germination represents a pivotal phase in crop production, exhibiting pronounced sensitivity to abiotic stresses. In this study, wheat seeds of the 'Ningchun 4' variety were subjected to treatments involving zinc (Zn) chloride and iron (Fe) chloride, both individually and in combination. The impacts of these treatments on Fe and Zn accumulation, starch mobilization, antioxidant responses, and nitric oxide (NO) metabolism during seed germination were thoroughly examined. Individual application of Fe or Zn significantly inhibited and delayed wheat seed germination, which was accompanied by elevated levels of starch, sucrose, and soluble sugars, as well as increased reactive oxygen species and malondialdehyde concentrations. Concurrently, total amylase and α -amylase activities were downregulated, while antioxidant enzyme activities and the expression of *TaCAT*, *TaAPX*, and *TaGR* were upregulated. Seeds treated solely with Fe exhibited excessive Fe accumulation, heightened Fe^{2+} content, and diminished Zn content. Conversely, these trends were reversed in seeds treated with Zn alone. Furthermore, reduced NO levels were associated with downregulated nitrate reductase and nitric oxide synthase activities, alongside decreased expression of their corresponding genes in response to Fe exposure. Notably, the above effects induced by Zn alone were less severe compared to those induced by Fe stress. Importantly, the addition of Zn (100 μM or 250 μM) significantly alleviated the detrimental effects of Fe on several parameters in germinating seeds. The results from NO fluorescent probe staining corroborated the quantitative NO measurements across different treatments. In conclusion, an appropriate concentration of Zn effectively promoted the germination of Fe-stressed wheat seeds by mitigating Fe accumulation, attenuating oxidative damage, and enhancing starch mobilization during seed germination.

Keywords Seed germination, Iron, Zinc, Wheat seed, Starch mobilization

[†]Zhe Zhang, Rongrong Ma contributed equally to this work and should be regarded as co-first authors.

*Correspondence:

Yingli Yang

xbsfxbsdyang@163.com

¹College of Life Science, Northwest Normal University, Lanzhou 730070, PR China



© The Author(s) 2025. **Open Access** This article is licensed under a Creative Commons Attribution-NonCommercial-NoDerivatives 4.0 International License, which permits any non-commercial use, sharing, distribution and reproduction in any medium or format, as long as you give appropriate credit to the original author(s) and the source, provide a link to the Creative Commons licence, and indicate if you modified the licensed material. You do not have permission under this licence to share adapted material derived from this article or parts of it. The images or other third party material in this article are included in the article's Creative Commons licence, unless indicated otherwise in a credit line to the material. If material is not included in the article's Creative Commons licence and your intended use is not permitted by statutory regulation or exceeds the permitted use, you will need to obtain permission directly from the copyright holder. To view a copy of this licence, visit <http://creativecommons.org/licenses/by-nc-nd/4.0/>.

Introduction

Iron (Fe) and zinc (Zn) are essential micronutrients for seed germination and plant growth, serving as critical components of numerous functional proteins involved in physiological processes and material metabolism [1, 2]. However, environmental and agricultural pollution caused by excessive levels of these metals can severely inhibit crop germination, growth, and yield. For example, in regions such as Africa and Asia, Fe toxicity has been reported to reduce grain production by 12–100% [3, 4]. Additionally, seed germination in *Vigna radiata* is promoted by 100 $\mu\text{mol}\cdot\text{L}^{-1}$ Fe but inhibited at concentrations of 200–300 $\mu\text{mol}\cdot\text{L}^{-1}$ [5]. Furthermore, interactions between essential and non-essential elements are crucial for understanding heavy metal toxicity and developing mitigation strategies. Several previous studies have shown that exogenous nickel addition to copper (Cu)-stressed *Alyssum inflatum* seedlings significantly increases copper accumulation in both roots and shoots, resulting in synergistic growth inhibition [6], and that combined exposure to lead (Pb) and cadmium (Cd) exerts synergistic inhibitory effects on mulberry seed germination [7]. Our previous findings indicate that low-concentration zinc chloride (Zn) can partially alleviate oxidative damage induced by high-concentration Fe in wheat seedlings [8]. Despite these advances, studies on seed germination under combined heavy metal stress remain limited, highlighting the need for further investigation into the interactions between multiple metals and their impact on plant physiology.

The endogenous signaling molecule nitric oxide (NO) plays a pivotal role in plant and seed adaptation to abiotic stress [9]. For example, treatment with 2-phenyl-4,4,5,5-tetramethylimidazoline-1-oxyl-3-oxide (PTIO), an NO scavenger, has been shown to delay seed germination and reduce the germination rate (GR) in *Sorbus pohuashanensis* [10]. Conversely, exogenous NO application has been demonstrated to alleviate chromium (Cr) toxicity in tomato seeds, significantly enhancing the germination index (GI) and vigor index (VI) [9]. Similarly, the addition of sodium nitroprusside (SNP), an NO donor, mitigated the inhibitory effects of Cd on rice seed germination, accompanied by increased GR and VI [11]. These findings collectively highlight the active involvement of NO in regulating plant seed germination under stress conditions. In addition to NO, reactive oxygen species (ROS) play an essential role in plant seed germination. For instance, in *Helianthus annuus* seeds, germination is closely associated with the accumulation of superoxide anion ($\text{O}_2^{\cdot-}$) in the cotyledon and hydrogen peroxide (H_2O_2) in the radicle [12]. However, under adverse conditions such as heavy metal stress, the balance between ROS production and scavenging is disrupted, leading to excessive ROS accumulation that can inhibit seed

germination. For example, Ye et al. [13] demonstrated that Cu stress significantly increases $\text{O}_2^{\cdot-}$ and H_2O_2 levels during rice seed germination, concomitant with a reduction in GR. Similarly, Cd stress inhibits *Zea mays* L. seed germination while markedly elevating $\text{O}_2^{\cdot-}$ and H_2O_2 content [14]. To counteract excessive ROS accumulation and oxidative damage, plants have evolved complex ROS scavenging systems, including enzymatic mechanisms. Notably, exogenous NO application has been shown to counteract Cu-induced H_2O_2 elevation by enhancing the activities of catalase (CAT), peroxidase (POD), ascorbate peroxidase (APX), and superoxide dismutase (SOD) in wheat seeds, thereby alleviating the inhibitory effects of Cu stress on germination [15].

To date, the complex mechanisms underlying Fe toxicity in plants, particularly in crops and their seeds, remain poorly understood. In this study, we investigated the effects of high-concentration iron chloride (Fe, 500 μM) and optimal-concentration Zn (100 and 250 μM) treatments, applied individually or in combination, on Fe and Zn accumulation, sugar mobilization, NO production, and antioxidant responses during the germination of wheat (cultivar Ningchun-4) seeds. Our aim was to elucidate the mechanisms by which Fe inhibits wheat seed germination and to identify effective strategies for mitigating Fe toxicity during this critical developmental stage. This research holds significant theoretical and practical importance for understanding the agronomic impacts of high-concentration Fe stress and improving crop quality in Fe-polluted soils.

Materials and methods

Seed germination and treatment

Full and uniform wheat seeds were surface-sterilized by immersing in 0.1% (w/v) Mercuric Chloride solution for 8 min, followed by thorough rinsing with distilled water. The sterilized seeds were then placed in petri dishes and allowed to germinate in complete darkness at $25 \pm 1^\circ\text{C}$ in a controlled environment incubator. For the germination process, seeds in the control group were immersed with 1/4 strength Hoagland nutrient solution, while treatment groups were exposed to 1/4 strength Hoagland solution supplemented with either Fe, Zn, or their combinations. It is important to note that all seeds were maintained in a moist environment without complete submersion. The experimental design included six treatment groups with at least three biological replicates each: control (CK), 500 $\mu\text{mol}\cdot\text{L}^{-1}$ FeCl_3 , 100 $\mu\text{mol}\cdot\text{L}^{-1}$ ZnCl_2 , 250 $\mu\text{mol}\cdot\text{L}^{-1}$ ZnCl_2 , 500 $\mu\text{mol}\cdot\text{L}^{-1}$ FeCl_3 + 100 $\mu\text{mol}\cdot\text{L}^{-1}$ ZnCl_2 , 500 $\mu\text{mol}\cdot\text{L}^{-1}$ FeCl_3 + 250 $\mu\text{mol}\cdot\text{L}^{-1}$ ZnCl_2 .

The concentrations of Fe and Zn were determined based on our previous studies, such as Li et al. [16] and Xu et al. [17], as well as the study by Reis et al. [18]. Throughout the germination period (3 or 6 days), the

treatment solutions were refreshed every 48 h to maintain consistent nutrient and metal ion concentrations. Germinated seeds were collected at two critical time points (24 h and 72 h) for subsequent physiological and biochemical analyses.

Analyses of germination parameters

Fifty plump wheat seeds per petri dish, with four replicates, were germinated under dark conditions at 25 ± 1 °C for 6 days. Seed germination was defined as the point when the radicle reached 1 mm in length and broke through the seed coat. Throughout the germination period, the number of germinated seeds were recorded daily, and the radicle length was measured on the final day. Germination potential (GP), GR, GI, and VI were analyzed and calculated according to the method described by Ren et al. [19].

Fe and Zn staining and Fe^{2+} content measurement

The Fe content in germinated seeds was assessed using Perls staining, as described previously [20]. Briefly, seeds were immersed in Perls stain (4% hydrochloric acid (HCl) and 4% potassium ferrocyanide) for 2 h at 25 °C. Subsequently, the seeds were rinsed with distilled water and then treated with a methanol solution containing 10 mM sodium azide and 0.3% H_2O_2 for 1 h. Afterward, the seeds were washed with 100 mM potassium phosphate buffer (pH 7.4). Following this, the fortification reaction was carried out by incubating the seeds in a solution containing 3,3-diaminobenzidine (DAB) (0.025%, pH 7.4), H_2O_2 (0.005%), and cobalt chloride (0.005%) for 10–30 min. The stained seeds were observed under a microscope and photographed for further analysis.

The Fe^{2+} content was quantified using a ferrous colorimetric assay kit (Elabscience Biotechnology Co., Ltd.). Briefly, 0.1 g of wheat seeds was homogenized with 0.9 mL of extraction buffer and centrifuged at $12,000 \times g$ for 10 min. The resulting supernatant was collected, and its absorbance was measured at 593 nm to determine the Fe^{2+} concentration.

The Zn content in wheat seeds was determined using the dithizone (DTZ) method, which is based on the formation of a red-purple Zn-dithizonate complex [21]. Briefly, wheat seeds were soaked in a freshly prepared DTZ solution (500 mg/L 1,5-diphenylthiourea dissolved in methanol) for 30 min. After incubation, the excess solution on the seed surface was carefully removed, and the seeds were observed and photographed for further analysis.

Analysis of different sugar levels

Three sequential extractions of dry germinated seeds (0.1 g) were performed using distilled water (5 mL, 80 °C) for 30, 20, and 20 min, respectively. The extracts

were combined and diluted to a final volume of 25 mL to obtain the sugar extract. Following the method described by Hu et al. [22], 1 mL of the sugar extract was mixed with 4 mL of anthrone solution, and the absorbance was measured at 625 nm to determine the soluble sugar content. For sucrose quantification, 0.4 mL of the sugar extract was mixed with 0.2 mL of 2 M sodium hydroxide, 0.8 mL of 0.1% resorcinol, and 2.8 mL of 30% HCl, and the absorbance was recorded at 485 nm. The residual pellet from the initial extraction was further treated with distilled water and perchloric acid. After centrifugation ($4,000 \times g$, 10 min), the supernatant was adjusted to a final volume of 50 mL, and the starch content was measured using a method similar to that for soluble sugar. Sugar concentrations were expressed as $\text{mg}\cdot\text{g}^{-1}$ dry weight (DW).

Determination of amylase activity

Germinated seeds (0.5 g) were homogenized with 4 mL of distilled water and incubated at room temperature for 15 min with continuous shaking to ensure complete extraction. The homogenate was centrifuged at $3,000 \times g$ for 10 min, and the supernatant was collected as the stock solution. A diluted solution was prepared by mixing 1 mL of the stock solution with 9 mL of distilled water. For the assay, both control and test tubes containing 1 mL of either the stock solution or the diluted solution were incubated at 70 °C–40 °C, respectively, for 10 min. After rapid cooling, 2 mL of 3,5-dinitrosalicylic acid (DNS) reagent was added to the control tube. Both the control and test tubes were then incubated again at 40 °C for 10 min, followed by the addition of 1 mL of 1% amylase stock solution. After a 5-minute incubation at 40 °C, the reaction was terminated by the rapid addition of 2 mL of DNS solution. Finally, both sets of tubes were boiled for color development and then rapidly cooled. The absorbance at 540 nm was measured for both the control and test tubes. The activities of α -amylase and total amylase were expressed as $\text{U}\cdot\text{mg}^{-1}$ protein, as described previously [23].

Analyses of NO content and related enzyme activities

The NO content ($\mu\text{mol}\cdot\text{g}^{-1}$ FW) was determined following the method described by Murphy and Noack [24] with minor modifications. Briefly, germinated seeds (0.5 g) were homogenized in 50 mM Tris (hydroxymethyl) aminomethane hydrochloride (Tris-HCl) buffer (pH 7.4) containing 1 mM phenylmethyl sulfonyl fluoride (PMSF), 1 μM leupeptin, 320 mM sucrose, 1 mM dithiothreitol (DTT), 1 μM gastric inhibitory protein, 1 mM ethylenediaminetetraacetic acid (EDTA), and 0.1% polyvinylpyrrolidone (PVP). The homogenate was centrifuged at $10,000 \times g$ for 20 min, and the supernatant was collected. To eliminate endogenous ROS, the supernatant was co-incubated with 100 U of CAT and 100 U of SOD at

37 °C for 5 min. Subsequently, 4.5 mL of 5 mM oxygenated hemoglobin (HbO₂) was added, and the mixture was incubated at 25 °C for 2 min. The absorbance at 401 nm and 421 nm was measured to quantify the conversion of HbO₂ to methemoglobin.

The fluorescence localization of NO in germinated seeds was conducted using 3-amino,4-aminomethyl-2',7'-difluorescein, diacetate (DAF-FM DA) as described previously [25]. Briefly, germinated seeds were incubated in a solution containing 5 μM DAF-FM DA dissolved in dimethyl sulfoxide (DMSO) for 40 min at room temperature in the dark. After incubation, the seeds were rinsed at least three times with 10 mM sodium phosphate buffer (pH 7.4) to remove excess fluorescent dye from the seed surface. Fluorescence intensity was visualized using a Leica fluorescence microscope, with excitation and emission wavelengths set at 495 nm and 515 nm, respectively.

The activity of NR (U·mg⁻¹ protein) was determined according to the method described by Lea et al. [26]. Briefly, 1 g of wheat seeds was homogenized in 4 mL of 4-(2-hydroxyethyl)-1-piperazineethanesulfonic acid (HEPES) buffer (pH 7.5, 100 mM) containing 1 mM EDTA, 3% PVP, and 7 mM cysteine. The homogenate was centrifuged at 10,000 × g for 20 min to collect the supernatant for enzyme activity analysis. For the assay, 0.4 mL of the enzyme solution was mixed with 1.2 mL of 100 mM phosphate-buffered saline (PBS, pH 7.5) containing 2 mg·mL⁻¹ reduced coenzyme, and the reaction was allowed to proceed at 25 °C for 30 min. The reaction was terminated by adding 1 mL of 1% sulfanilamide, followed by the addition of 1 mL of 0.2% alpha-naphthylamine for color development. After 15 min of incubation, the absorbance at 540 nm was measured.

The activity of NOS (U·mg⁻¹ protein) was determined following the method described by Murphy's method [24] with minor modifications. Briefly, 1 g of wheat seeds was homogenized in 5 mL of extraction buffer containing 50 mM Tris-HCl (pH 7.5), 200 μM PMSE, 7 mM reduced glutathione, and 500 μM EDTA. The homogenate was centrifuged at 9,000 × g for 30 min, and an appropriate volume of the supernatant was mixed with 4.5 mL of 5 mM oxygenated hemoglobin. The absorbance at 401 nm and 421 nm was measured to quantify NOS activity.

Analyses of malondialdehyde (MDA) and ROS levels

The MDA level was determined according to the method described by Li et al. [27]. Briefly, 0.5 g of germinated seeds was homogenized in 5 mL of 0.25% thiobarbituric acid (TBA) solution. The homogenate was boiled for 30 min and then cooled to room temperature. After centrifugation at 10,000 × g for 10 min, the absorbance of the supernatant was measured at 450 nm, 532 nm, and 600 nm to calculate the MDA concentration.

The localization of H₂O₂ and O₂⁻ in germinated seeds was performed using DAB and Nitroretetrazolium blue chloride (NBT) staining, respectively, following the methods described by Ruan et al. [28]. Briefly, germinated seeds were immersed in a staining solution containing either DAB (1 mg·mL⁻¹) or NBT (0.5 mg·mL⁻¹) and incubated at 25 °C in the dark for 6 h. After incubation, excess dye on the seed surface was removed by rinsing with distilled water, and images were captured for further analysis.

The H₂O₂ content was determined following the method described by Velikova et al. [29]. Briefly, 0.5 g of wheat seeds was homogenized in 5 mL of 0.1% trichloroacetic acid in an ice bath and centrifuged at 12,000 × g for 20 min. Subsequently, 0.7 mL of the supernatant was mixed with 0.7 mL of PBS (10 mM, pH 7.0) and 1.4 mL of 1 M potassium iodide. The mixture was incubated in the dark for 30 min, and the absorbance at 370 nm was measured to quantify H₂O₂ content.

Wheat seeds (0.5 g) were homogenized in 3 mL of PBS (pH 7.8, 50 mM) containing 1 mM EDTA. The homogenate was centrifuged at 12,000 × g for 20 min, and 1 mL of the supernatant was mixed with 0.1 mL of 10 mM hydroxylamine hydrochloride. The mixture was incubated at 25 °C for 60 min. Subsequently, 1 mL of 17 mM p-aminobenzenesulfonic acid and 1 mL of 7 mM α-naphthylamine were added sequentially. After color development at room temperature for 20 min, the absorbance at 530 nm was measured to determine the O₂⁻ concentration, as described previously [28].

The hydroxyl radical (·OH) content was analyzed according to the method described by Liu et al. [30]. Briefly, wheat seeds (0.1 g) were homogenized in 1 mL of PBS (pH 7.4, 10 mM) containing 2 mM 2-deoxy-D-ribose. The homogenate was centrifuged at 12,000 × g for 15 min, and 200 μL of the supernatant was incubated at 37 °C for 2 h. Subsequently, 3 mL of 0.5% TBA and 1 mL of acetic acid were added to the supernatant. The mixture was boiled for 30 min and then cooled at 4 °C for 10 min. The absorbance at 532 nm was measured to determine the ·OH content.

Analyses of antioxidant enzyme activity

The extraction of antioxidant enzymes was performed following the method described by He et al. [31]. Briefly, germinated seeds (0.5 g) were homogenized in 2 mL of PBS (pH 7.8, 50 mM) containing 0.1% PVP and 0.1 mM EDTA. The homogenate was centrifuged at 12,000 × g for 30 min, and the supernatant was collected for the determination of enzyme activity.

SOD activity was determined by mixing 50 μL of the enzyme solution with 3 mL of PBS (pH 7.8, 50 mM) containing 2 mM riboflavin, 100 μM EDTA, 75 μM NBT, and 13 mM methionine. The reaction mixture was

illuminated for 30 min, and the absorbance at 560 nm was measured. A blank control, which was not exposed to illumination, was used for comparison. One unit (U) of SOD activity was defined as the amount of enzyme required to inhibit 50% of NBT reduction under the assay conditions.

POD activity was determined by mixing 50 µL of the enzyme solution with 3 mL of PBS (50 mM, pH 7.0) containing 20 mM guaiacol. The reaction was initiated by adding 0.25% H₂O₂. The increase in absorbance at 470 nm was recorded every 20 s for a total duration of 2 min. One U of POD activity was defined as the amount of enzyme required to produce a change in absorbance of 0.01 per min at 470 nm.

CAT activity was determined by mixing 100 µL of the enzyme solution with 3 mL of PBS (50 mM, pH 7.0). The reaction was initiated by adding 0.25% H₂O₂. The decrease in absorbance at 240 nm was recorded every 20 s for a total duration of 2 min. One U of CAT activity was defined as the amount of enzyme required to produce a change in absorbance of 0.01 per min at 240 nm.

APX activity (U·mg⁻¹ protein) was determined following the method described by Zhong et al. [32]. Briefly, 0.5 g of wheat seeds was homogenized in 5 mL of PBS (50 mM, pH 7.0) containing 1 mM ascorbic acid (AsA) and 1 mM EDTA in an ice bath. The homogenate was centrifuged at 13,000 × g for 20 min, and the supernatant was collected. For the assay, 100 µL of the supernatant was mixed with 3 mL of PBS (50 mM, pH 7.0) and 500 µM AsA, and the mixture was pre-incubated at 25 °C for 5 min. The reaction was initiated by adding 5% H₂O₂. APX activity was determined by measuring the decrease in absorbance at 290 nm.

GR activity was determined as follows. Briefly, 0.5 g of wheat seeds was homogenized in 50 mM Tris-HCl buffer

(pH 7.5) containing 0.1% PVP and 100 mM EDTA at low temperature. The homogenate was centrifuged at 13,000 × g for 30 min at 4 °C, and the supernatant was collected. For the assay, 150 µL of the supernatant was mixed with 3 mL of reaction buffer (50 mM Tris-HCl, pH 7.5) containing 500 µM oxidized glutathione GSSG, 150 µM reduced nicotinamide adenine dinucleotide phosphate, and 3 mM magnesium chloride. The absorbance at 340 nm was measured after the reaction reached completion, as described previously [31].

All antioxidant enzyme activity were expressed as U·mg⁻¹ protein.

Determination of relative gene expression

Total RNA was extracted from germinated seeds using a plant total RNA extraction kit, following the method described by Zhang et al. [33]. Reverse transcription of RNA was performed using the PrimeScript™ RT Reagent Kit with gDNA Eraser (Takara, Perfect Real Time). Gene-specific primers, listed in Table 1, were synthesized by Shanghai Sheng Gong Biological Engineering Co., Ltd. Quantitative PCR (qPCR) was carried out using the SYBR Premix Ex Taq™ kit (Takara). The wheat glyceraldehyde-3-phosphate dehydrogenase gene (*TaGAPDH*) was used as the reference gene, and the relative gene expression levels were calculated using the 2^{-ΔΔC_t} method.

Statistical analysis

Statistical analysis of the experimental data was performed using Excel 2022 and SPSS 20.0 software, while graphs were generated and processed using Origin 2018 and Adobe Photoshop CS6. The results are presented as means ± standard error (SE). Seed germination parameters were derived from at least four replicates, while other indicators were obtained from at least three replicates. Significant differences between groups (*P* ≤ 0.05) were determined using one-way analysis of variance (ANOVA) followed by Duncan's multiple range test.

Results

Germination parameter under different treatments

As shown in Fig. 1, the application of Fe or Zn alone significantly inhibited wheat seed germination, with the most pronounced inhibition observed at 500 µM Fe and the least at 250 µM Zn. Under 500 µM Fe and 100 µM Zn treatments, GP decreased to approximately 67% and 87% of the control, and GR reduced by approximately 38%, 25%, and 17%, respectively, compared to the control. Similar trends were observed for the GI and VI in seeds treated with Fe, 100 µM Zn, or 250 µM Zn alone. Notably, the addition of Zn significantly enhanced GP, GR, GI, and VI in Fe-treated seeds. For instance, seeds exposed to Fe + 100 µM Zn exhibited increases of approximately

Table 1 Primers used for RT-qPCR

Primer	Sequences (5'–3')
<i>TaGAPDH</i>	F: TTAGACTTGCGAAGCCAGCA R: AAATGCCCTTGAGGTTTCCC
<i>TaNR</i>	F: GGCAACTTCGTCATCAAC R: CATCTCCGTCTCGTCCTC
<i>TaNOS</i>	F: ACGCTGATGATCTGCCTTCT R: TCTGTGGTGCGGACCATATT
<i>TaSOD</i>	F: CTGGAAGAACCTCAAGCCTATC R: GATCCTTGTAAGCACCTCTG
<i>TaPOD</i>	F: CTTGACACGCGCTACTACAC R: GGTGGACGCAAGTTCC
<i>TaCAT</i>	F: CAACCACTACGACGGGCTCA R: GGGCTGCTTGAAGTTGTTCTCC
<i>TaAPX</i>	F: CAGTGGCCAGCATCTACAA R: TAGCCCGCGATAACTACAGC
<i>TaGR</i>	F: CTTCCATCCGCCCTTCA R: TCGCATCTGTTTCACCC

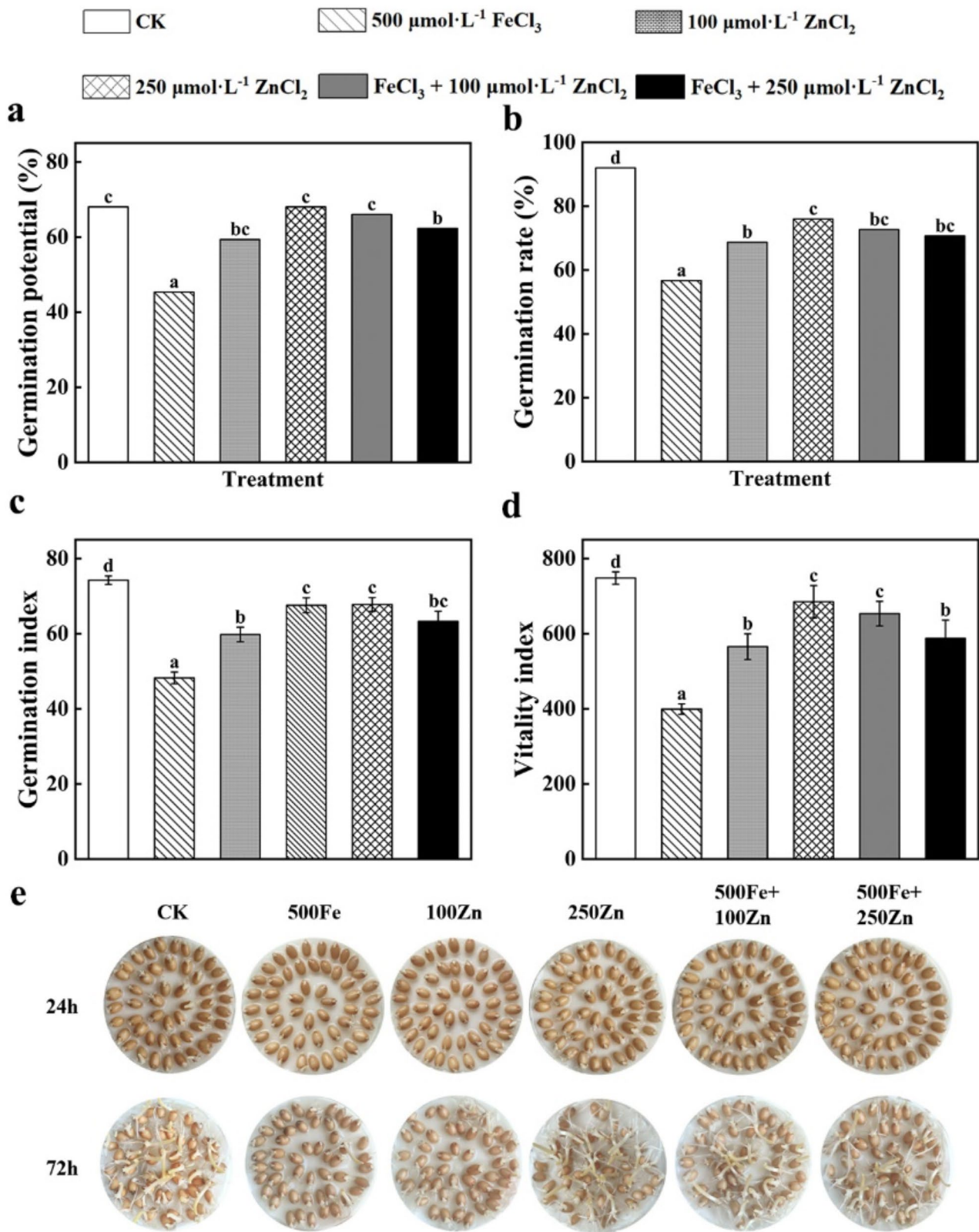


Fig. 1 Changes of germination parameters under Zn and Fe alone and combination treatments. Data represent the values of the mean \pm SE (standard error) of three replicates. Note Different lowercase letters indicate significant differences between treatments under the same indicator ($p < 0.05$)

46%, 28%, 41%, and 64% in GP, GR, GI, and VI, respectively, compared to those treated with Fe alone.

Fe and Zn levels under different treatments

As shown in Fig. 2a and d, Fe staining of seeds was most intense in response to Fe exposure alone and the least intense to Zn alone, both in early and delayed germination stages. Furthermore, the application of 100 μM or 250 μM Zn significantly reduced Fe staining in Fe-stressed seeds, with reductions of approximately 95% and 80% observed in seeds treated with Fe + 100 μM Zn and Fe + 250 μM Zn, respectively, compared to those treated with Fe alone.

Further analysis revealed that Fe^{2+} levels in 24-hour- and 72-hour-germinated seeds under Fe treatment increased significantly by 9% and 350%, respectively, compared to the control (Fig. 2b). In contrast, this parameter in 24-hour-germinated seeds decreased markedly by approximately 35% and 33% under 100 μM and 250 μM Zn treatments alone, respectively, but remained unchanged in 72-hour-germinated seeds. Compared to Fe treatment alone, the combined exposure of Fe + Zn (100 μM or 250 μM) significantly reduced Fe^{2+} levels in both early- and delayed-germinated seeds, with no significant difference observed between Fe + 100 μM Zn and Fe + 250 μM Zn.

In all germinated seeds, Zn staining was significantly weaker in Fe-stressed seeds than that in untreated ones, but was the most intense in 250 μM Zn-exposed seeds. Compared to Fe treatment alone, Zn (100 or 250 μM) application significantly enhanced Zn staining in Fe-stressed wheat seeds, and a higher staining was due to 250 μM Zn addition. Additionally, under the same germination environment, Zn staining in early germinated seeds was weaker than that in delayed germinated ones (Fig. 2c and e).

Sugar content under different treatments

Exposure to Fe or Zn alone significantly increased starch, sucrose, and soluble sugar levels in all germinated seeds, with higher levels observed in Fe-exposed seeds compared to Zn-exposed seeds (Table 2). The addition of Zn to Fe-exposed seeds negatively impacted starch, sucrose, and soluble sugar levels. For instance, in 24-hour-germinated seeds, these parameters decreased by approximately 11%, 25%, and 15% under Fe + 100 μM Zn exposure and by 27%, 10%, and 29% under Fe + 250 μM Zn exposure, respectively, compared to Fe treatment alone. Notably, under different treatments, sucrose and soluble sugar levels were lower in 24-hour-germinated seeds than in 72-hour-germinated seeds.

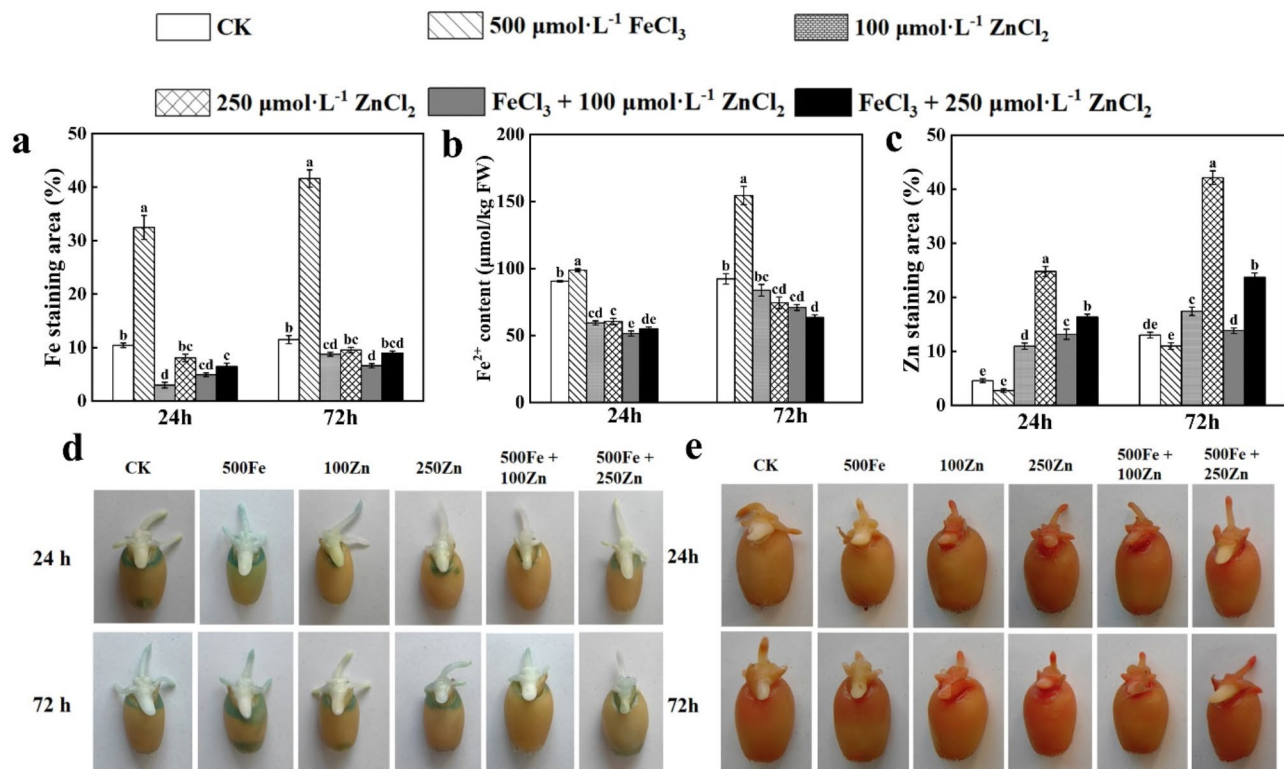


Fig. 2 Changes of Fe^{2+} level, Zn and Fe staining under Zn and Fe alone and combination treatments. Data represent the values of the mean \pm SE (standard error) of three replicates. Note Different lowercase letters indicate significant differences between treatments under the same indicator ($p < 0.05$)

Table 2 Changes of starch, sucrose, soluble sugar content ($\text{mg}\cdot\text{g}^{-1}$ DW) and amylase activity ($\text{U}\cdot\text{mg}^{-1}$ protein) under Zn and Fe alone and combination treatments. Data represent the values of the mean \pm se (standard error) of three replicates. Note different lowercase letters indicate significant differences between treatments under the same indicator ($p < 0.05$). CK: control; 500 FeCl_3 : 500 $\mu\text{mol}\cdot\text{L}^{-1}$ FeCl_3 ; 100 ZnCl_2 : 100 $\mu\text{mol}\cdot\text{L}^{-1}$ ZnCl_2 ; 250 ZnCl_2 : 250 $\mu\text{mol}\cdot\text{L}^{-1}$ ZnCl_2

	Treatment time	CK	500 FeCl_3	100 ZnCl_2	250 ZnCl_2	FeCl_3 + 100 ZnCl_2	FeCl_3 + 250 ZnCl_2
Starch content	24 h	31.64 \pm 0.24 a	83.03 \pm 0.36 e	31.81 \pm 0.35 a	54.74 \pm 0.40 b	73.86 \pm 0.37 d	60.86 \pm 0.54 c
	72 h	28.70 \pm 0.33 a	64.33 \pm 0.42 d	41.37 \pm 1.83 b	43.34 \pm 1.21 b	57.66 \pm 2.03 c	57.72 \pm 1.94 c
Sucrose content	24 h	4.50 \pm 0.24 a	8.50 \pm 0.21 d	6.80 \pm 0.25 b	6.84 \pm 0.29 b	6.42 \pm 0.27 b	7.67 \pm 0.16 c
	72 h	3.95 \pm 0.08 a	9.11 \pm 0.12 e	7.13 \pm 0.10 b	7.34 \pm 0.16 b	7.78 \pm 0.15 c	8.34 \pm 0.18 d
Soluble sugar content	24 h	31.34 \pm 1.50 d	53.06 \pm 1.50 a	37.32 \pm 1.44 c	42.81 \pm 1.69 b	45.11 \pm 2.12 b	37.70 \pm 1.34 c
	72 h	53.63 \pm 2.80 d	83.26 \pm 3.70 a	63.38 \pm 2.16 c	72.83 \pm 1.66 b	73.71 \pm 2.03 b	62.71 \pm 2.85 c
Total amylase activity	24 h	1.33 \pm 0.05 a	0.32 \pm 0.02 e	0.97 \pm 0.03 b	0.57 \pm 0.01 d	0.54 \pm 0.01 d	0.76 \pm 0.02 c
	72 h	0.46 \pm 0.03 a	0.20 \pm 0.01 e	0.39 \pm 0.02 b	0.28 \pm 0.02 d	0.27 \pm 0.01 d	0.34 \pm 0.01 c
α -amylase activity	24 h	0.15 \pm 0.01 a	0.05 \pm 0.01 e	0.13 \pm 0.01 b	0.09 \pm 0.00 c	0.06 \pm 0.01 de	0.07 \pm 0.01 cd
	72 h	0.18 \pm 0.01 a	0.07 \pm 0.01 c	0.15 \pm 0.01 a	0.08 \pm 0.01 bc	0.08 \pm 0.00 bc	0.10 \pm 0.01 b

Amylase activity under different treatments

Further analysis was conducted to evaluate total amylase and α -amylase activities in germinated seeds under different treatments. As shown in Table 2, total amylase and α -amylase activities were significantly reduced in seeds exposed to 500 μM Fe or 100 and 250 μM Zn individually, with the lowest enzyme activity observed under Fe treatment and the highest under 250 μM Zn exposure. For instance, total amylase activity decreased by approximately 76%, 93%, and 57%, while α -amylase activity decreased by 65%, 16%, and 43% under 500 μM Fe, 100 μM Zn, and 250 μM Zn treatments, respectively, compared to the control. Additionally, the application of 100 μM or 250 μM Zn positively influenced total amylase and α -amylase activities in Fe-treated seeds, with a stronger effect observed at 250 μM Zn compared to 100 μM Zn. It was also noted that 24-hour-germinated seeds exhibited higher total amylase activity but lower α -amylase activity than 72-hour-germinated seeds.

NO metabolism under different treatments

NO levels in all germinated seeds were significantly reduced under Fe treatment alone but remained unchanged under 100 μM Zn treatment (Fig. 3a). In contrast, this parameter in seeds exposed to 250 μM Zn were not significantly altered in 24-hour-germinated seeds but were markedly reduced in 72-hour-germinated seeds. Except for a notable increase in NO content in 72-hour-germinated seeds, the application of 100 μM or 250 μM Zn had no significant effect on NO levels in Fe-treated seeds. Additionally, NO fluorescence staining showed reduced fluorescence intensity in germinated seeds under Fe exposure, compared to the control, but no change under Zn treatment alone. Notably, Zn + Fe treatment resulted in stronger NO staining compared to Fe treatment alone. Moreover, NO fluorescence intensity was higher in 24-hour-germinated seeds than in

72-hour-germinated seeds under the same treatment conditions (Fig. 3b).

NR and NOS activities, as well as *TaNR* and *TaNOS* gene expression, were significantly reduced in all germinated seeds under Fe treatment alone (Fig. 3c–f). Differently, in 24-hour-germinated seeds, NR activity and *TaNR* expression remained unaltered under 100 μM or 250 μM Zn treatment alone, in 72-hour-germinated seeds, NOS activity remained unchanged whereas NR activity and *TaNOS* expression decreased under 100 μM or 250 μM Zn treatment. Additionally, except for insignificant changes in 72-hour-germinated seeds treated with Fe + 100 μM Zn, NR activity and *TaNR* expression increased significantly under Fe + Zn (100 μM or 250 μM) treatment compared to Fe treatment alone. Differently, NOS activity and *TaNOS* expression increased significantly in 72-hour-germinated seeds treated with Fe + 100 μM Zn but showed no significant changes under other treatments.

MDA and ROS contents under different treatments

As shown in Fig. 4, MDA levels increased to approximately 272%, 108%, and 185% of the control in seeds germinated for 24 h, and to about 285%, 143% and 170% of the control for 72 h, respectively, following treatment with 500 μM Fe, 100 μM Zn, and 250 μM Zn. Compared to Fe treatment alone, the addition of Zn (100 or 250 μM) partially mitigated the Fe-induced increase in MDA content in germinated seeds, although no significant change was observed in 24-hour-germinated seeds treated with Fe + 100 μM Zn (Fig. 4a).

Except for negligible changes in H_2O_2 levels in 24-hour-germinated seeds exposed to 100 μM Zn and $\cdot\text{OH}$ levels in 72-hour-germinated seeds exposed to 100 μM Zn, treatment with Fe or Zn alone significantly promoted ROS generation in germinated seeds, with the highest levels observed under 500 μM Fe treatment, and the smallest increases occurred under 100 μM Zn treatment.

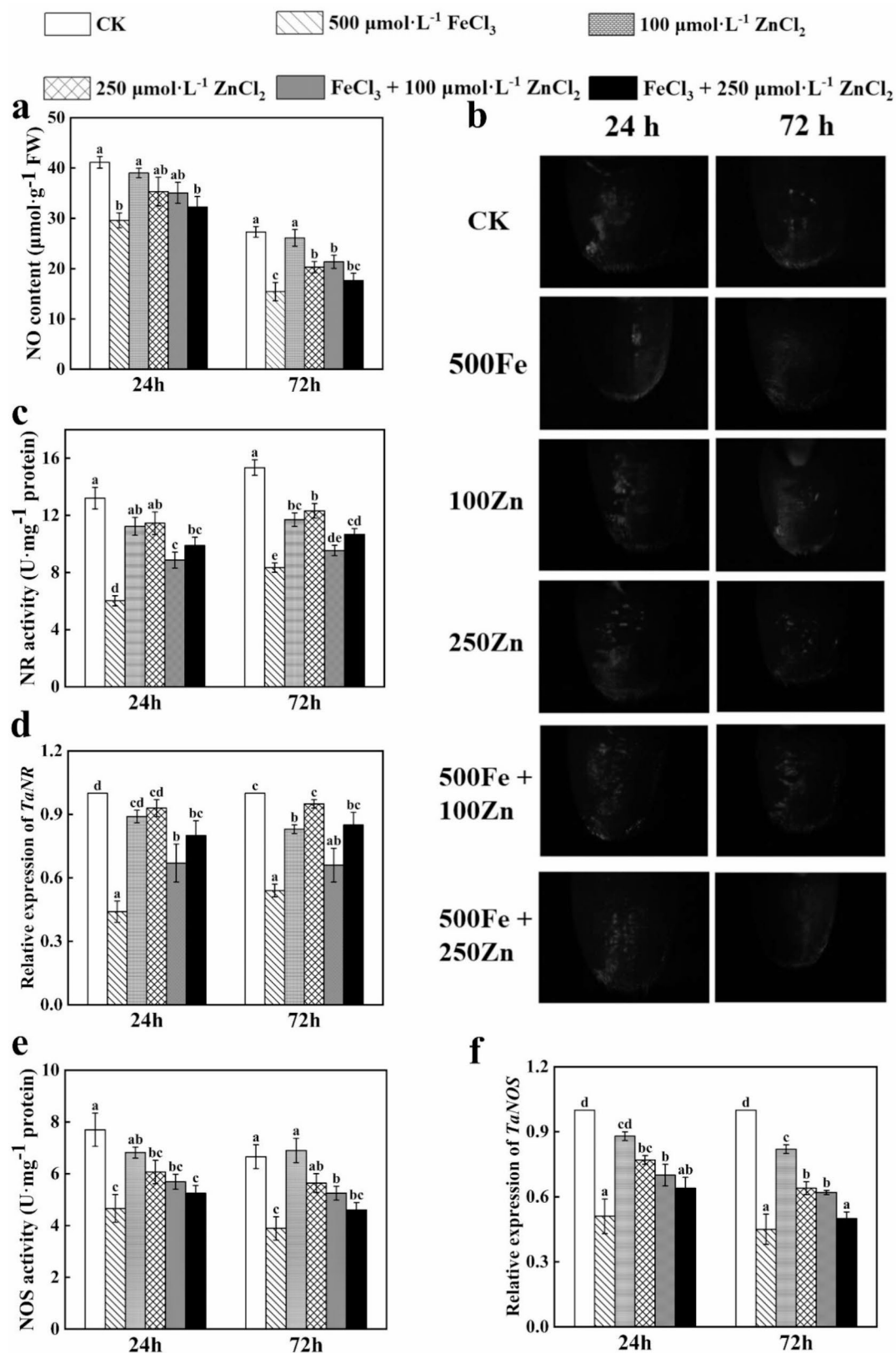


Fig. 3 Changes of nitric oxide anabolism under Zn and Fe alone and combination treatments. Data represent the values of the mean \pm SE (standard error) of three replicates. Note Different lowercase letters indicate significant differences between treatments under the same indicator ($p < 0.05$)

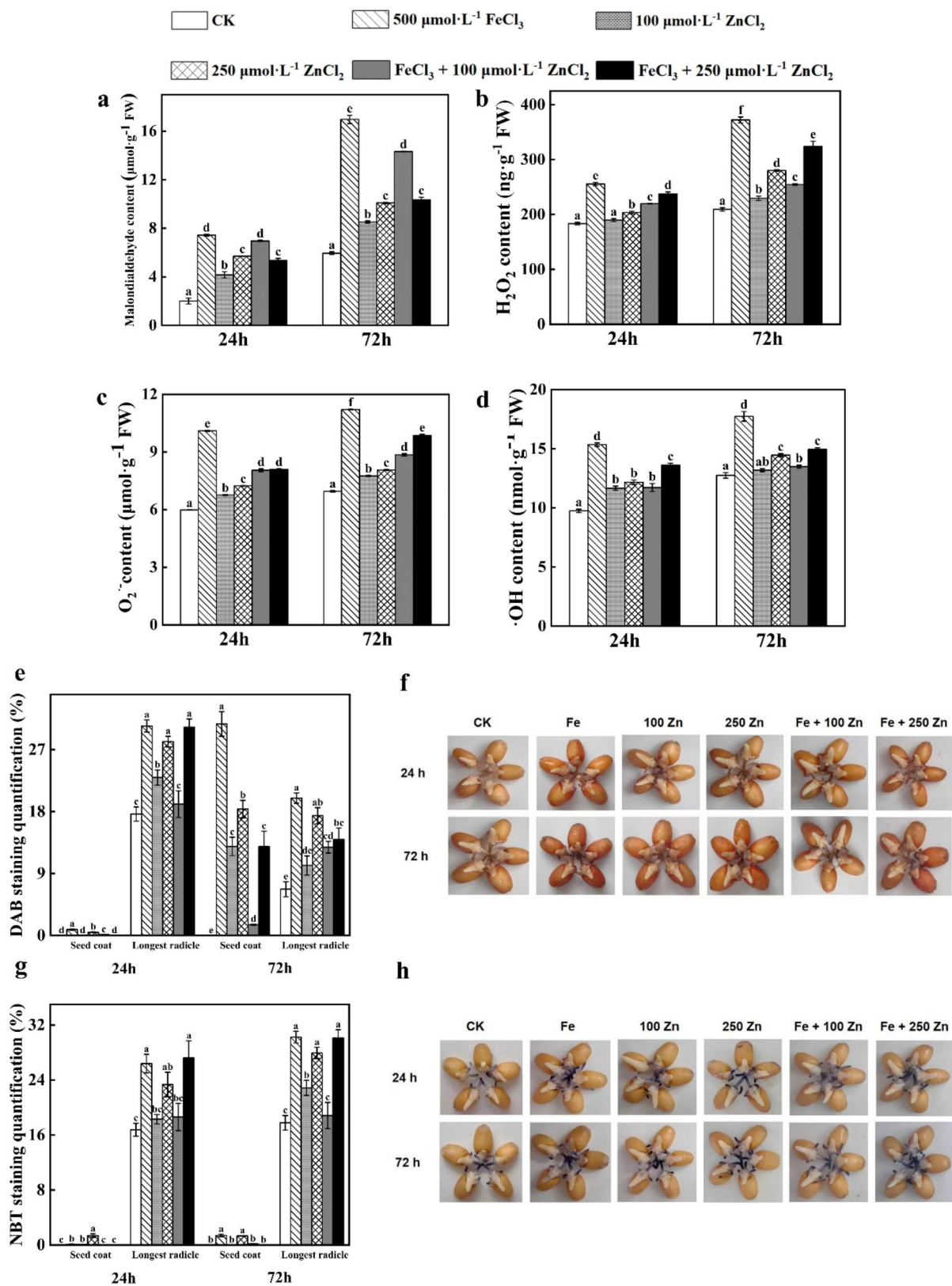


Fig. 4 Changes of MDA content and ROS levels under Zn and Fe alone and combination treatments. Data represent the values of the mean \pm SE (standard error) of three replicates. Note Different lowercase letters indicate significant differences between treatments under the same indicator ($p < 0.05$)

Furthermore, the levels of these three ROS parameters were consistently higher in seeds germinated for 72 h than in those germinated for 24 h. Additionally, the application of Zn at 100 or 250 μM effectively mitigated the Fe-induced increase in $\text{O}_2^{\cdot-}$, H_2O_2 , and $\cdot\text{OH}$ levels in all germinated seeds, with the effect of 100 μM Zn being more pronounced than that of 250 μM Zn (Fig. 4b–d).

The localization of H_2O_2 and $\text{O}_2^{\cdot-}$ in germinated seeds was further investigated through histochemical staining (Fig. 4e–f). Both individual Fe and Zn treatments (100 and 250 μM) significantly enhanced the accumulation of H_2O_2 and $\text{O}_2^{\cdot-}$ in the seed coat and primary radicle, as evidenced by DAB and NBT staining, respectively. Notably, Fe treatment induced the most pronounced accumulation of these two parameters in the seed coat, and the 100 μM Zn treatment showed minimal effects on DAB staining in the seed coat and NBT staining in the primary radicle. Importantly, co-application of Zn (100 or 250 μM) substantially reduced the accumulation of both H_2O_2 and $\text{O}_2^{\cdot-}$ in both the seed coat and primary radicle of germinated seeds. Furthermore, comparative analysis revealed that delayed-germinated seeds consistently exhibited significantly higher levels of both H_2O_2 and $\text{O}_2^{\cdot-}$ accumulation compared to early-germinated seeds under identical treatment conditions.

Antioxidant enzyme activities and their gene expression under different treatments

As shown in Table 3, treatment with Fe alone did not significantly alter the activities of POD and SOD in germinated seeds. However, it upregulated CAT, APX, and GR activities to approximately 2.01-, 1.87-, and 2.19-fold of the control in seeds germinated for 24 h, and to 1.49-, 1.71-, and 2.05-fold in seeds germinated for 72 h, respectively. Compared to the control, 100 μM Zn exposure alone enhanced SOD activity in all germinated seeds and POD activity in 72-hour-germinated seeds, but had

no significant effect on CAT, APX, or GR activity. In contrast, treatment with 250 μM Zn alone positively influenced the activities of all five enzymes (SOD, POD, CAT, APX, and GR) in both 24-hour- and 72-hour-germinated seeds. Furthermore, POD, APX, and SOD activities were consistently higher in 24-hour-germinated seeds than in those germinated for 72 h. Additionally, SOD activity remained unchanged in seeds treated with Fe + 100 μM Zn but significantly increased in seeds treated with Fe + 250 μM Zn. Conversely, POD activity markedly increased in all germinated seeds under Fe + Zn treatment compared to Fe-alone treatment. Compared to Fe treatment alone, the addition of 100 μM or 250 μM Zn under Fe treatment further downregulated CAT, APX, and GR activities in seeds germinated for 24 h. However, except for a significant decrease in CAT and GR activities in seeds germinated for 72 h, these three enzyme activity did not significantly alter Fe + Zn treatment compared with Zn exposure alone.

Compared with the control, *TaSOD* and *TaPOD* expression remained downregulated but *TaCAT*, *TaAPX*, and *TaGR* expression significantly upregulated approximately 23%, 48% and 44% in all germinated seeds under Fe-alone-treatment, respectively. Different from Fe treatment, Zn treatment alone did not affect these gene expression in germinated seeds, except for significant increases of *TaSOD* expression under 100 μM Zn treatment and *TaPOD* expression under 250 μM Zn treatment in 24 h-germinated seeds. Compared to Fe treatment alone, Zn application significantly upregulated *TaSOD* and *TaPOD* expression but had no effect on *TaAPX* expression. In contrast to these three genes, *TaCAT* and *TaGR* expression in Fe-stressed seeds was significantly downregulated by 100 μM Zn application but remained unchanged with 250 μM Zn application. Individual Fe stress markedly suppressed *TaSOD* and *TaPOD* expression while significantly enhanced *TaCAT*, *TaAPX*, and

Table 3 Changes of antioxidant enzyme activities ($\text{U}\cdot\text{mg}^{-1}$ protein) under Zn and Fe alone and combination treatments. Data represent the values of the mean \pm se (standard error) of three replicates. Note different lowercase letters indicate significant differences between treatments under the same indicator ($p < 0.05$). CK: control; 500 FeCl_3 : 500 $\mu\text{mol}\cdot\text{L}^{-1}$ FeCl_3 ; 100 ZnCl_2 : 100 $\mu\text{mol}\cdot\text{L}^{-1}$ ZnCl_2 ; 250 ZnCl_2 : 250 $\mu\text{mol}\cdot\text{L}^{-1}$ ZnCl_2

	Treatment time	CK	500 FeCl_3	100 ZnCl_2	250 ZnCl_2	FeCl_3 + 100 ZnCl_2	FeCl_3 + 250 ZnCl_2
SOD activity	24 h	107.39 \pm 2.75 cd	105.41 \pm 1.67 d	116.94 \pm 0.56 b	125.40 \pm 3.96 a	108.46 \pm 1.58 cd	114.04 \pm 1.58 bc
	72 h	71.72 \pm 1.97 c	69.80 \pm 2.65 c	81.11 \pm 1.79 ab	87.12 \pm 2.11 a	75.38 \pm 1.14 bc	78.41 \pm 1.96 b
POD activity	24 h	81.65 \pm 1.14 bc	77.00 \pm 1.96 c	87.55 \pm 1.02 b	94.97 \pm 3.61 a	85.24 \pm 1.48 b	83.24 \pm 2.12 bc
	72 h	34.02 \pm 1.35 cd	29.85 \pm 2.79 d	53.97 \pm 2.19 b	66.23 \pm 4.37 a	42.94 \pm 2.77 c	40.07 \pm 2.68 c
CAT activity	24 h	6.79 \pm 0.34 d	13.68 \pm 0.41 a	7.88 \pm 0.13 cd	11.58 \pm 0.74 b	8.62 \pm 0.52 c	12.71 \pm 0.59 ab
	72 h	7.66 \pm 0.37 b	11.41 \pm 0.50 a	7.77 \pm 0.38 b	12.15 \pm 0.47 a	4.57 \pm 0.44 c	8.38 \pm 0.81 b
APX activity	24 h	10.16 \pm 0.78 e	19.01 \pm 1.75 a	10.84 \pm 0.80 de	14.86 \pm 1.76 bc	14.22 \pm 1.58 cd	18.53 \pm 1.12 ab
	72 h	9.47 \pm 0.50 c	16.22 \pm 0.74 a	9.38 \pm 0.44 c	13.00 \pm 0.78 b	9.57 \pm 0.57 c	14.41 \pm 1.03 ab
GR activity	24 h	4.64 \pm 0.51 d	10.18 \pm 0.93 a	5.19 \pm 0.60 d	7.68 \pm 0.54 bc	6.22 \pm 0.64 cd	9.21 \pm 0.61 ab
	72 h	4.93 \pm 0.40 c	10.12 \pm 0.56 a	5.64 \pm 0.40 c	7.38 \pm 0.69 b	4.44 \pm 0.29 c	7.40 \pm 0.43 b

TaGR expression in germinated seeds, except that *TaAPX* expression, remained unaltered in seeds germinated for 72 h (Table 4).

Correlation analysis

In seeds germinated for 24 and 72 h, NO content, NOS activity, and *TaNOS* expression exhibited a negative correlation with H_2O_2 , $O_2^{\cdot-}$, $\cdot OH$, and MDA levels, but a positive correlation with *TaSOD* and *TaPOD* expression. Furthermore, in all germinated seeds, NR and NOS activities, as well as *TaNOS* expression, were negatively associated with APX and GR activities and *TaAPX* expression. ROS generation and MDA levels were also negatively correlated with SOD and POD activities. Notably, a strong negative correlation was observed between ROS and MDA levels and *TaSOD* and *TaPOD* expression. Additionally, a significant positive relationship was detected between NR, NOS and their corresponding genes, as well as between antioxidant enzyme activities and their gene expression (Fig. 5).

Discussion

Seed germination is highly sensitive to environmental changes, and parameters such as GP, GI, and VI are widely used to assess the impact of adverse conditions on seed germination [34]. In this study, exposure to 500 μM Fe or 100, 250 μM Zn significantly reduced GP, GR, GI, and VI in wheat seeds, with the most pronounced reduction observed under Fe stress and the weakest effect associated with 250 μM Zn treatment. Notably, individual Zn treatment resulted in negligible changes in GP. Consistent with the effects of Fe treatment alone, previous studies have shown that $FeSO_4$ (at concentrations exceeding 14 mM) and Fe (62 μM) significantly reduced GR and germination coefficients in various plant seeds [18, 35], accompanied by excessive Fe accumulation [18]. Similarly, our findings revealed that Fe-alone-stressed seeds

exhibited extreme Fe accumulation, increased Fe^{2+} content, and reduced Zn content, whereas Zn-alone-treated seeds displayed low Fe and Fe^{2+} levels alongside elevated Zn content. These observations suggest the presence of competitive transport mechanisms between Fe and Zn and indicate that excessive Fe accumulation may be a key factor underlying the inhibitory effects of Fe on wheat seed germination. In contrast to the response of wheat seeds, the GR and/or radicle length of rice seeds were significantly enhanced under $FeSO_4$ treatment (18–36 mM or 3.6 mM) [36, 37], and Zn exposure at 734 μM had minimal effects on *Brassica juncea* L. seed germination [38]. These differences highlight that the effects of heavy metals on seed germination depend on plant species, metal type, and treatment concentration. Importantly, various mitigation strategies for heavy metal toxicity have been reported in different plant species. For example, melatonin (MT) or SNP application has been shown to alleviate Cr-induced reductions in GR, GI, and VI in crop and vegetable seeds [39, 40], primarily by reducing Cr or Pb accumulation [37, 40]. Additionally, Fe application significantly enhanced the GR of *Oryza sativa* L. seeds under Pb stress [37]. However, few studies have focused on mitigating Fe toxicity during seed germination. The present study demonstrated that the addition of 100 or 250 μM Zn significantly improved GR, GP, GI, and VI in Fe-treated seeds compared to Fe-alone-treated seeds, accompanied by reduced Fe content and increased Zn content. These findings suggest that appropriate Zn concentrations may alleviate the inhibitory effects of Fe toxicity on wheat seed germination by preventing excessive Fe accumulation.

During seed germination, soluble sugars serve as essential substrates for the expansion and growth of embryonic cells [37]. Previous studies have reported that Cd treatment significantly increases soluble sugar content, including sucrose, during the germination of bean seeds

Table 4 Changes of antioxidant enzyme gene expression under Zn and Fe alone and combination treatments. Data represent the values of the mean \pm se (standard error) of three replicates. Note different lowercase letters indicate significant differences between treatments under the same indicator ($p < 0.05$). CK: control; 500 $FeCl_3$: 500 $\mu mol \cdot L^{-1}$ $FeCl_3$; 100 $ZnCl_2$: 100 $\mu mol \cdot L^{-1}$ $ZnCl_2$; 250 $ZnCl_2$: 250 $\mu mol \cdot L^{-1}$ $ZnCl_2$

	Treatment time	CK	500 $FeCl_3$	100 $ZnCl_2$	250 $ZnCl_2$	$FeCl_3$ + 100 $ZnCl_2$	$FeCl_3$ + 250 $ZnCl_2$
<i>TaSOD</i>	24 h	1.00 \pm 0.00 bc	0.59 \pm 0.06 d	1.33 \pm 0.10 a	1.21 \pm 0.08 ab	0.75 \pm 0.08 cd	1.20 \pm 0.12 ab
	72 h	1.00 \pm 0.00 a	0.30 \pm 0.08 e	0.88 \pm 0.12 ab	0.74 \pm 0.07 bc	0.54 \pm 0.07 cd	0.47 \pm 0.07 de
<i>TaPOD</i>	24 h	1.00 \pm 0.00 b	0.56 \pm 0.10 c	1.20 \pm 0.11 ab	1.35 \pm 0.07 a	1.09 \pm 0.08 ab	1.36 \pm 0.07 a
	72 h	1.00 \pm 0.00 ab	0.36 \pm 0.05 c	1.13 \pm 0.07 a	1.00 \pm 0.07 ab	0.82 \pm 0.08 b	1.03 \pm 0.08 ab
<i>TaCAT</i>	24 h	1.00 \pm 0.00 b	1.23 \pm 0.06 a	1.04 \pm 0.08 ab	1.13 \pm 0.06 ab	1.02 \pm 0.06 b	1.17 \pm 0.07 ab
	72 h	1.00 \pm 0.00 b	1.22 \pm 0.05 a	1.04 \pm 0.03 b	1.22 \pm 0.06 a	0.82 \pm 0.06 c	0.98 \pm 0.06 b
<i>TaAPX</i>	24 h	1.00 \pm 0.00 b	1.48 \pm 0.19 a	1.08 \pm 0.09 ab	1.31 \pm 0.12 ab	1.26 \pm 0.11 ab	1.31 \pm 0.13 ab
	72 h	1.00 \pm 0.00 ab	1.29 \pm 0.14 a	0.82 \pm 0.13 b	1.07 \pm 0.09 ab	0.96 \pm 0.05 ab	1.23 \pm 0.12 a
<i>TaGR</i>	24 h	1.00 \pm 0.00 bc	1.44 \pm 0.17 a	0.85 \pm 0.07 c	1.25 \pm 0.11 ab	1.04 \pm 0.06 bc	1.37 \pm 0.05 a
	72 h	1.00 \pm 0.00 c	1.36 \pm 0.07 a	0.86 \pm 0.05 c	1.11 \pm 0.08 bc	1.01 \pm 0.06 c	1.28 \pm 0.13 ab

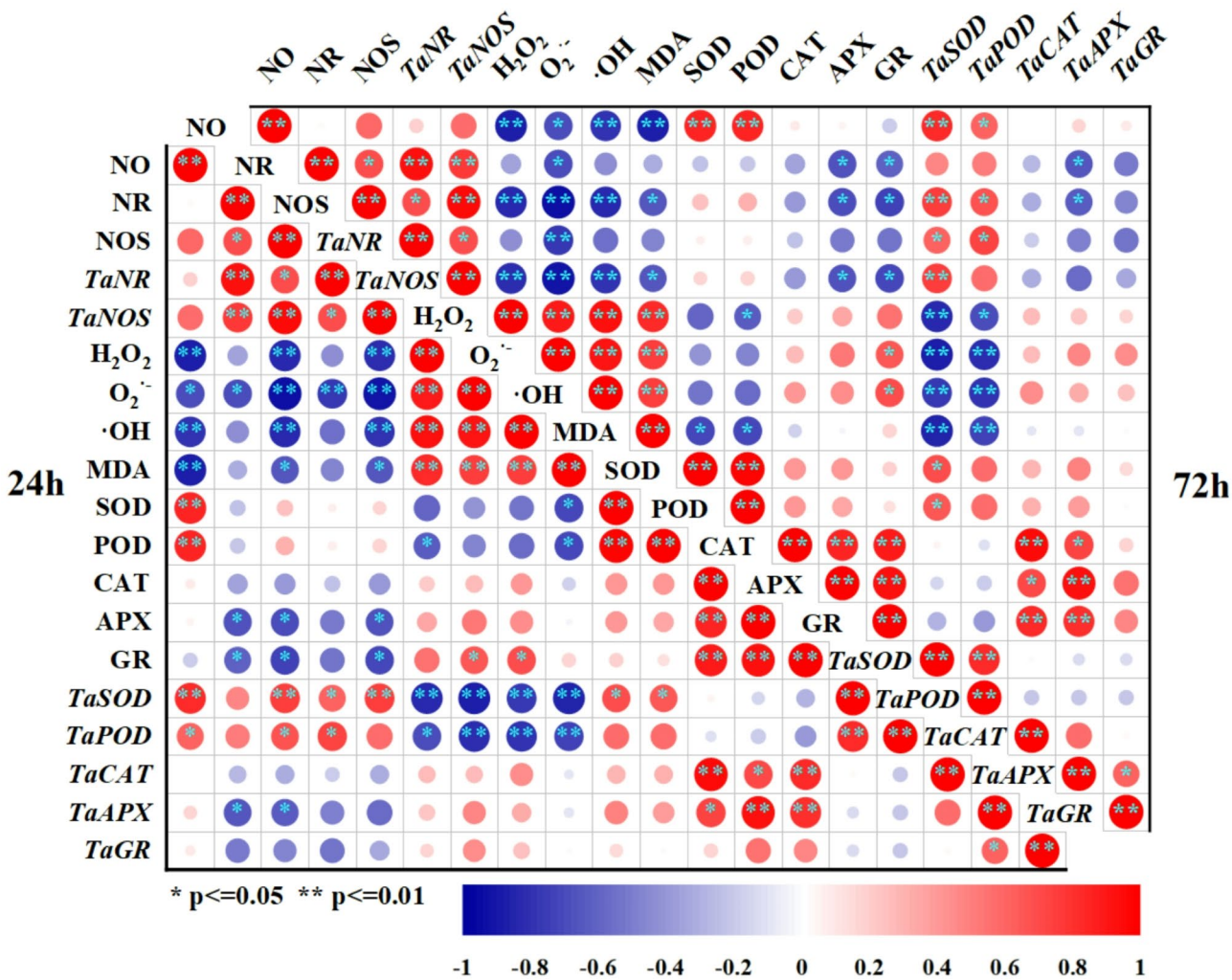


Fig. 5 Correlation analysis between NO generation and antioxidant response. Data represent the values of the mean ± SE (standard error) of three replicates. Note Different lowercase letters indicate significant differences between treatments under the same indicator ($p < 0.05$)

[41]. Similarly, in this study, individual treatment with 500 μM Fe or 100, 250 μM Zn significantly elevated soluble sugar, sucrose, and starch levels in all germinated seeds. Notably, these parameters were markedly higher in seeds germinated for 72 h compared to those germinated for 24 h, indicating a delayed energy supply from carbohydrate decomposition in seeds treated with Fe or Zn alone. This delay likely contributes to the observed inhibition and delay in seed germination. Amylase plays a critical role in seed germination by catalyzing starch catabolism to provide energy for the embryo and radicle to break through the seed coat [39]. Nabaei and Amooaghaie [42] demonstrated that Cd stress reduced soluble sugar content and inhibited α - and β -amylase activities in *Catharanthus roseus* seeds, concomitant with suppressed seed germination. Similarly, the inhibition of seed germination and α -amylase activity has been observed in wheat seeds [39] and tomato seeds [40] under Cr stress, alongside impaired mobilization of reserve substances,

including starch. In this study, the inhibition and delay of wheat seed germination under individual Fe or Zn treatment were associated with the downregulation of total amylase and α -amylase activities. Additionally, amylase activities were higher in seeds germinated for 24 h compared to those germinated for 72 h across all treatments. Importantly, the application of Zn (100 or 250 μM) significantly alleviated the inhibitory effects of Fe on these parameters during wheat seed germination. Consistent with our findings, enhanced β -amylase activity has been linked to improved germination of *Oryza sativa* L. seeds under Fe application during Pb stress [37]. Based on these observations, we conclude that an increased energy supply derived from sugar degradation enhances seed germination under combined Zn and Fe treatment.

NO plays a crucial role in regulating plant amylase activity, sugar metabolism [40, 42], and seed germination [15, 43]. For instance, a significant reduction in NO content during the germination of tomato seeds under Cr

stress has been associated with decreased GR, GI, and VI [40]. Similarly, salinity stress negatively affects NO content and seed germination in *Sorbus pohuashanensis* [44]. However, few studies have investigated the activity of NO synthases, including NR and NOS, during seed germination under heavy metal stress. In this study, changes in NO levels, NR and NOS activities, and their gene expression in germinated seeds revealed that the inhibition of NR and NOS collectively contributes to reduced NO synthesis in Fe-treated wheat seeds. In contrast, under salt and alkali stress, NR activity gradually increased alongside NO content during the germination of catalpa tree seeds, while NOS activity initially decreased and then rose with prolonged germination time [44]. Furthermore, we observed that the reduction in these parameters was more pronounced in delayed-germinated seeds compared to early-germinated ones, suggesting that decreased NO content may be a key factor underlying the inhibition and delay of wheat seed germination under high Fe stress. This conclusion is supported by a previous study demonstrating that exogenous NO application promotes tomato seed germination by enhancing NO content and upregulating NR activity under Cr toxicity [40]. Unlike Fe-stressed seeds, negligible changes in NO levels and NOS activity in Zn-treated seeds indicated that NO might not play a significant role in Zn-induced retardation of wheat seed germination. Moreover, insignificant changes in NO levels, NOS activity, and *TaNOS* expression were observed in seeds treated with Zn + Fe compared to those treated with Fe alone, further suggesting that the promotion of seed germination by Zn application is likely independent of NO production in Fe-stressed wheat seeds. This finding aligns with a previous study showing that pre-soaking with SNP did not affect GP or GI in rice seeds under Cd stress [31]. Additionally, increased NO levels coupled with marked inhibition of seed germination have been reported in *Medicago sativa* [45] and *Arabidopsis thaliana* [46] under NaCl treatment.

Abiotic stresses, including heavy metals, can induce excessive ROS accumulation, leading to membrane lipid peroxidation and even cell death [47]. To mitigate oxidative stress, plants activate both enzymatic and non-enzymatic ROS scavenging systems [48]. Key antioxidant enzymes, such as SOD, POD, CAT, APX, and GR, play critical roles in ROS detoxification, protecting membrane integrity and maintaining cellular redox homeostasis [48]. SOD, a metalloprotein, converts $O_2^{\cdot-}$ into oxygen and H_2O_2 , while CAT and POD further decompose H_2O_2 into water and oxygen [49]. APX and GR, integral components of the ascorbate-glutathione cycle, interact with antioxidants to scavenge ROS. Hu et al. [15] reported that Cu-induced inhibition of wheat seed germination is accompanied by elevated MDA and H_2O_2 levels, as well

as increased POD and APX activities. Similarly, prolonged germination in rice seeds under Cu stress corresponds to increased MDA and H_2O_2 content, enhanced CAT and APX activities, and upregulated expression of *OsCATa*, *OsCATb*, and *OsCATc* genes [13]. Consistent with these observations, the present study demonstrated that treatment with 500 μ M Fe, 100 μ M Zn, or 250 μ M Zn alone significantly increased MDA content in seeds germinated for both 24 and 72 h, with the most pronounced effect observed under Fe treatment and the weakest effect under 100 μ M Zn treatment. The levels of H_2O_2 and $O_2^{\cdot-}$ in plants or seeds can be visualized using DAB and NBT staining [28]. In this study, DAB and NBT staining of the seed coat and radicle was more intense under 500 μ M Fe or 250 μ M Zn treatment compared to 100 μ M Zn treatment, and was more pronounced in seeds germinated for 72 h than in those germinated for 24 h. These observations confirm that high H_2O_2 and $O_2^{\cdot-}$ accumulation caused stronger oxidative damage in Fe-stressed wheat seeds compared to Zn-treated seeds. Notably, although elevated $O_2^{\cdot-}$, H_2O_2 , and $\cdot OH$ levels induced oxidative damage in wheat seeds, the increased activities of antioxidant enzymes, including SOD, POD, CAT, APX, and GR, as well as the upregulation of *TaCAT*, *TaAPX*, and *TaGR* expression, contributed to ROS elimination in seeds treated with Fe or Zn. This explains why Fe-stressed seeds accumulated higher ROS and MDA levels than Zn-treated seeds. Therefore, the delay or inhibition of wheat seed germination induced by Fe or Zn can be attributed to ROS accumulation and subsequent oxidative damage. In contrast, Cr treatment results in increased MDA, $O_2^{\cdot-}$, and H_2O_2 levels but downregulated SOD, POD, APX, and CAT activities, as well as *TaSOD2*, *TaPOD*, *TaAPX*, and *TaCAT* expression during wheat seed germination [39]. Similarly, Pb-induced retardation of seed germination in *Pinus sylvestris* and maize seeds is associated with increased MDA, $O_2^{\cdot-}$, and H_2O_2 levels, alongside reduced SOD, POD, and CAT activities [49, 50]. Furthermore, a previous study has shown that 100 μ M MT application improves the activities of POD, SOD, APX, CAT, and GR, while reducing the accumulation of MDA, H_2O_2 , and $O_2^{\cdot-}$, thereby alleviating the adverse effects of Cu stress on rice seed germination [51]. Research by Zhang et al. [50] revealed that exogenous application of imidazole and dimethylthiourea significantly reduced H_2O_2 accumulation and suppressed seed germination, while considerably increasing CAT and SOD activities during maize seed germination under Pb stress. Additionally, Li et al. [52] demonstrated that exogenous MT application enhances the GR of rice seeds by increasing SOD, POD, APX, CAT, and GR activities and significantly decreasing MDA, H_2O_2 , and $O_2^{\cdot-}$ levels. In the present study, we observed that the enhancement of SOD and POD activities, along with the reduction of CAT, APX, and GR

activities and their gene expression, in Fe + Zn-treated seeds corresponded to decreased ROS and MDA levels compared to Fe-alone-treated seeds. These findings indicate that Zn addition alleviates the inhibitory effects of Fe toxicity on wheat seed germination by reducing ROS accumulation and oxidative damage induced by Fe stress.

Conclusion

This study demonstrated that impaired starch mobilization and enhanced oxidative damage are likely associated with Fe- or Zn-induced inhibition of wheat seed germination. The weakened starch mobilization under individual Fe or Zn treatment was attributed to the downregulation of total amylase and α -amylase activities in germinated seeds. Further investigations revealed that Fe-alone-stressed seeds exhibited excessive Fe accumulation, increased Fe²⁺ content, and reduced Zn content, whereas these trends were reversed in Zn-alone-treated seeds. Additionally, reduced NO levels were correlated with downregulated NR and NOS activities, as well as decreased expression of their corresponding genes in response to Fe exposure. Although elevated levels of O₂^{•-}, H₂O₂, and •OH induced oxidative damage in wheat seeds, the increased activities of antioxidant enzymes, including SOD, POD, CAT, APX, and GR, along with the upregulation of *TaCAT*, *TaAPX*, and *TaGR* gene expression, contributed to ROS scavenging in seeds treated with Fe or Zn. Notably, the adverse effects induced by Zn alone were less pronounced compared to those caused by Fe stress. Importantly, the addition of Zn (100 μ M or 250 μ M) significantly alleviated the detrimental effects of Fe on several parameters in germinating seeds. These findings suggest that an appropriate concentration of Zn effectively promotes the germination of Fe-stressed wheat seeds by reducing Fe accumulation, mitigating oxidative damage, and enhancing starch mobilization during seed germination. The present study provides both theoretical and practical insights into the application of Zn for improving plant tolerance to Fe stress environments.

Acknowledgements

National Natural Science Foundation of China (NO. 32160749).

Author contributions

Data test, write articles and revision: Z Z; Data test and write article: RR M; Provide information and write article: YH T; Revise article: ZL W; Design experiment and the corresponding author: YL Y.

Data availability

No datasets were generated or analysed during the current study.

Declarations

Competing interests

The authors declare no competing interests.

Published online: 04 April 2025

References

- Cvitanich C, Przybyłowicz WJ, Urbanski DF, Jurkiewicz AM, Mesjasz-Przybyłowicz J, Blair MW, Astudillo C, Jensen EØ, Stougaard J. Iron and ferritin accumulate in separate cellular locations in *Phaseolus* seeds. BMC Plant Biol. 2010;10:26.
- Su L, Xie J, Wen W, Li J, Zhou P, An Y. Interaction of zinc and IAA alleviate aluminum-induced damage on photosystems via promoting proton motive force and reducing proton gradient in alfalfa. BMC Plant Biol. 2020;20(1):433.
- Sikirou M, Shittu A, Konaté KA, Maji AT, Ngaujah AS, Sanni KA, Ogunbayo SA, Akintayo I, Saito K, Dramé KN. Screening African rice (*Oryza glaberrima*) for tolerance to abiotic stresses: I. Fe toxicity. Field Crops Res. 2016;220:3–9.
- Becker M, Asch F. Iron toxicity in rice—conditions and management concepts. J Plant Nutr Soil Sci. 2005;168:558–73.
- Verma L, Verma L, Verma L, Pandey N. The effect of Fe toxicity on seed germination and early seedling growth of green gram (*Vigna radiata* L. Wilczek). J Plant Growth Regul. 2017;6:1427–30.
- Ghasemi R, Ghaderian SM, Krämer U. Interference of nickel with copper and iron homeostasis contributes to metal toxicity symptoms in the nickel hyperaccumulator plant *Alyssum inflatum*. New Phytol. 2009;184(3):566–80.
- Si L, Zhang J, Hussain A, Qiao Y, Zhou J, Wang X. Accumulation and translocation of food chain in soil-mulberry (*Morus Alba* L.)-silkworm (*Bombyx mori*) under single and combined stress of lead and cadmium. Ecotox Environ Saf. 2021;208(15):111582.
- Ma T, Duan XH, Yang YL, Gao TP. Zinc-alleviating effects on iron-induced phytotoxicity in roots of *Triticum aestivum* L. Biol Plant. 2017;61(4):733–40.
- Khan MN, Alamri S, Al-Amri AA, Alsubaie QD, Al-Munqedi B, Ali HM, Pratap V, Siddiqui MH. Effect of nitric oxide on seed germination and seedling development of tomato under chromium toxicity. J Plant Growth Regul. 2021;40(6):2358–70.
- Yang L, Zhang DY, Liu HN, Wei C, Wang JA, Shen HL. Effects of a nitric oxide donor and nitric oxide scavengers on *Sorbus pahuashanensis* embryo germination. J Res. 2018;29(3):631–8.
- He JY, Ren YF, Chen XL. Protective roles of nitric oxide on seed germination and seedling growth of rice (*Oryza sativa* L.) under cadmium stress. Ecotox Environ Saf. 2014;108:114–9.
- Oracz K, El-maarouf-bouteau H, Kranner I, Bogatek R, Corbineau F, Bailly C. The mechanisms involved in seed dormancy alleviation by hydrogen cyanide unravel the role of reactive oxygen species as key factors of cellular signaling during germination. Plant Physiol. 2009;150(1):494–505.
- Ye NH, Li HX, Zhu GH, Liu YG, Liu R, Xu WF, Jing Y, Peng XX, Zhang JH. Copper suppresses abscisic acid catabolism and catalase activity, and inhibits seed germination of rice. Plant Cell Physiol. 2014;55(11):2008–16.
- Chen JL, Zeng XY, Yang WJ, Xie HJ, Ashraf U, Mo ZW, Liu JH, Li GK, Li W. Seed priming with multiwall carbon nanotubes (MWCNTs) modulates seed germination and early growth of maize under cadmium (Cd) toxicity. J. Soil sci. Plant Nutr. 2021;21:1793–805.
- Hu KD, Hu LY, Li YH, Zhang FQ, Zhang H. Protective roles of nitric oxide on germination and antioxidant metabolism in wheat seeds under copper stress. Plant Growth Regul. 2007;53:173–83.
- Li X, Ma H, Jia P, Wang J, Jia L, Zhang T, Yang Y, Chen H, Wei X. Responses of seedling growth and antioxidant activity to excess iron and copper in *Triticum aestivum* L. Ecotoxicol Environ Saf. 2012;86:47–53.
- Xu YL, Guo JY, Zhang Z, Ma RR, Ma H, Zhang Y, Yang YL. Chloroplast antioxidant reactions associated with zinc-alleviating effects on iron toxicity in wheat seedlings. Photosynthetica. 2024;62:381–92.
- Reis S, Pavia I, Carvalho A, Moutinho-Pereira J, Correia C, Lima-Brito J. Seed priming with iron and zinc in bread wheat: effects in germination, mitosis and grain yield. Protoplasma. 2018;255:1179–94.
- Ren Y, Wang W, He J, Zhang LY, Wei YJ, Yang M. Nitric oxide alleviates salt stress in seed germination and early seedling growth of Pakchoi (*Brassica chinensis* L.) by enhancing physiological and biochemical parameters. Ecotox Environ Saf. 2020;187(15):109785.
- Roschztardt H, Conéjéro G, Curie C, Mari S. Straightforward histochemical staining of Fe by the adaptation of an old-school technique: identification of the endodermal vacuole as the site of Fe storage in Arabidopsis embryos. Plant Signal Behav. 2010;5(1):56–7.

Received: 25 December 2024 / Accepted: 24 March 2025

21. Ozturk L, Yazici MA, Yucel C, Torun A, Cekic C, Bagci A, Ozkan H, Braun H, Sayers Z, Cakmak I. Concentration and localization of zinc during seed development and germination in wheat. *Physiol Plant*. 2006;128(1):144–52.
22. Hu YM, Zhang P, Zhang X, Liu YQ, Feng SS, Guo DW. Multi-Wall carbon nanotubes promote the growth of maize (*Zea mays*) by regulating carbon and nitrogen metabolism in leaves. *J Agric Food Chem*. 2021;69(17):4981–91.
23. Zhang Y, Qiao D, Zhang Z, Li YP, Shi SQ, Yang YL. Calcium signal regulated carbohydrate metabolism in wheat seedlings under salinity stress. *Physiol Mol Biol Plants*. 2024;30:123–36.
24. Murphy ME, Noack E. Nitric oxide assay using hemoglobin method. *Methods Enzymol*. 1994;233:240–50.
25. Yang F, Ding F, Duan X, Zhang J, Li XN, Yang YL. ROS generation and proline metabolism in calli of halophyte *Nitratia tangutorum* Bobr. To sodium Nitroprusside treatment. *Protoplasma*. 2014;251:71–80.
26. Lea US, Hoopen FT, Provan F, Kaiser WM, Meyer C, Lillo C. Mutation of the regulatory phosphorylation site of tobacco nitrate reductase results in high nitrite excretion and NO emission from leaf and root tissue. *Planta*. 2004;219:59–65.
27. Li HP, Sun HC, Ping WC, Liu LT, Zhang YJ, Zhang K, Bai ZY, Li AC, Zhu JJ, Li CD. Exogenous ethylene promotes the germination of cotton seeds under salt stress. *J Plant Growth Regul*. 2023;42:3923–33.
28. Ruan MJ, He WL, He R, Wang XX, Wei JX, Zhu YJ, Li RL, Jiang ZJ, Na XF, Wang XM, Bi YR. Alternative oxidase 2 influences Arabidopsis seed germination under salt stress by modulating ABA signalling and ROS homeostasis. *Environ Exp Bot*. 2024;217:105568.
29. Velikova V, Yordanov I, Edreva RA. Oxidative stress and some antioxidants in acid rain-treated bean plants. *Plant Sci*. 2000;151(1):59–66.
30. Liu YJ, Zhao ZG, Si J, Di CX, Han J, An LZ. Brassinosteroids alleviate chilling-induced oxidative damage by enhancing antioxidant defense system in suspension cultured cells of *Chorispora Bungeana*. *Plant Growth Regul*. 2009;59:207–14.
31. He JY, Ren YF, Chen XL, Chen H. Protective roles of nitric oxide on seed germination and seedling growth of rice (*Oryza sativa* L.) under cadmium stress. *Ecotox Environ Saf*. 2014;108:114–9.
32. Zhong WX, Xie CC, Hu D, Pu SY, Xiong X, Ma J, Sun LX, Huang Z, Jiang MY, Li X. Effect of 24-epibrassinolide on reactive oxygen species and antioxidative defense systems in tall fescue plants under lead stress. *Ecotoxicol Environ Saf*. 2020;187(15):109831.
33. Zhang Y, Li GY, Si LB, Liu N, Gao TP, Yang YL. Effects of tea polyphenols on the activities of antioxidant enzymes and the expression of related gene in the leaves of wheat seedlings under salt stress. *Environ Sci Pollut Res*. 2021;28:65447–61.
34. Nanda R, Agrawal V. Elucidation of zinc and copper induced oxidative stress, DNA damage and activation of defence system during seed germination in *Cassia angustifolia* Vahl. *Environ Exp Bot*. 2016;125:31–41.
35. Hatamzadeh A, Sharaf ARN, Vafaei MH, Salehi M, Ahmadi G. Effect of some heavy metals (Fe, Cu and Pb) on seed germination and incipient seedling growth of *Festuca rubra* Ssp. *Commute* (Chewings fescue). *Intl J Agri Crop Sci*. 2012;4(15):1068–73.
36. Kharb V, Sharma V, Dhaliwal SS, Kalra A. Influence of iron seed priming on seed germination, growth and iron content in rice seedlings. *J Plant Nutr*. 2023;46:4054–62.
37. Wang LL, Liu BT, Wang YB, Qin YC, Zhou YF, Qiao H. Influence and interaction of iron and lead on seed germination in upland rice. *Plant Soil*. 2020;455:187–202.
38. Wang N, Ren J, Wang LL, Wang YH, Wang Z, Guo D. A preliminary study to explain how *Streptomyces pactum* (Act12) works on phytoextraction: soil heavy metal extraction, seed germination, and plant growth. *Environ Monit Assess*. 2023;195:757.
39. Lei KQ, Sun SZ, Zhong KT, Li SY, Hu H, Sun CJ, Zheng QM, Tian ZW, Dai TB, Sun JY. Seed soaking with melatonin promotes seed germination under chromium stress via enhancing reserve mobilization and antioxidant metabolism in wheat. *Ecotox Environ Saf*. 2021;220(1):112241–50.
40. Khan MN, Alamri S, Al-Amri AA, Alsubaie QD, Al-Munqedi B, Ali HM, Singh VP, Singh MH. Effect of nitric oxide on seed germination and seedling development of tomato under chromium toxicity. *J Plant Growth Regul*. 2021;40:2358–70.
41. Sfaxi-bousbih A, Chaoui A, Ferjani EE. Cadmium impairs mineral and carbohydrate mobilization during the germination of bean seeds. *Ecotox Environ Saf*. 2010;73(6):1123–9.
42. Nabaei M, Amooaghaie R. Interactive effect of melatonin and sodium Nitroprusside on seed germination and seedling growth of *Catharanthus roseus* under cadmium stress. *Russ J Plant Physiol*. 2019;66:128–39.
43. Li XN, Jiang HD, Liu FL, Cai J, Dai TB, Cao WX, Jiang D. Induction of chilling tolerance in wheat during germination by pre-soaking seed with nitric oxide and Gibberellin. *Plant Growth Regul*. 2013;71:31–40.
44. Wang YT, Zhao CH, Wang XD, Shen HL, Yang L. Exogenous ethylene alleviates the inhibition of *Sorbus pohuashanensis* embryo germination in a saline-alkali environment (NaHCO₃). *Int J Mol Sci*. 2023;24(4):4244–57.
45. Wang YQ, Li L, Cui WT, Xu S, Shen WB, Wang R. Hydrogen sulfide enhances alfalfa (*Medicago sativa*) tolerance against salinity during seed germination by nitric oxide pathway. *Plant Soil*. 2012;351:107–19.
46. Lin YC, Yang L, Paul M, Zu YG, Tang ZY. Ethylene promotes germination of Arabidopsis seed under salinity by decreasing reactive oxygen species: evidence for the involvement of nitric oxide simulated by sodium Nitroprusside. *Plant Physiol Biochem*. 2013;73:211–8.
47. Wei LJ, Zhang J, Wang CL, Liao WB. Recent progress in the knowledge on the alleviating effect of nitric oxide on heavy metal stress in plants. *Plant Physiol Biochem*. 2020;147:161–71.
48. Shah K, Nahakpam S. Heat exposure alters the expression of SOD, POD, APX and CAT isozymes and mitigates low cadmium toxicity in seedlings of sensitive and tolerant rice cultivars. *Plant Physiol Biochem*. 2012;57:106–13.
49. Staszak AM, Malecka A, Ciereszko I, Ratajczak E. Differences in stress defence mechanisms in germinating seeds of *Pinus sylvestris* exposed to various lead chemical forms. *PLoS ONE*. 2020;15(9):e0238448.
50. Zhang YF, Deng BL, Li ZT. Inhibition of NADPH oxidase increases defense enzyme activities and improves maize seed germination under Pb stress. *Ecotox Environ Saf*. 2018;158:187–92.
51. Li RQ, Wu LQ, Shao YF, Hu QW, Zhang HL. Melatonin alleviates copper stress to promote rice seed germination and seedling growth via crosstalk among various defensive response pathways. *Plant Physiol Biochem*. 2022;179:65–77.
52. Li R, Zheng W, Yang R, Hu Q, Ma L, Zhang H. *OsSGT1* promotes melatonin-ameliorated seed tolerance to chromium stress by affecting the *OsABI5-OsAPX1* transcriptional module in rice. *Plant J*. 2022;112(1):151–71.

Publisher's note

Springer Nature remains neutral with regard to jurisdictional claims in published maps and institutional affiliations.